AIP | Applied Physics Letters

Solid-state nuclear magnetic resonance analysis of phase separation behavior of regioregular poly(3-hexylthiophene) and [6,6]-phenyl-C61-butyric acid methyl ester in bulk heterojunction organic solar cells

Tatsuya Fukushima, Hironobu Kimura, Yurie Shimahara, and Hironori Kaji

Citation: Appl. Phys. Lett. **99**, 223301 (2011); doi: 10.1063/1.3662854
View online: http://dx.doi.org/10.1063/1.3662854
View Table of Contents: http://apl.aip.org/resource/1/APPLAB/v99/i22
Published by the American Institute of Physics.

Solid-state nuclear magnetic resonance analysis of phase separation behavior of regioregular poly(3-hexylthiophene) and [6,6]-phenyl-C_{61}-butyric acid methyl ester in bulk heterojunction organic solar cells

Tatsuya Fukushima, Hironobu Kimura, Yurie Shimahara, and Hironori Kaji[a)]
Institute for Chemical Research, Kyoto University, Uji, Kyoto 611-0011, Japan

(Received 27 August 2011; accepted 20 October 2011; published online 30 November 2011)

The origin of the improvement in power conversion efficiency (PCE) by the thermal annealing of bulk heterojunction organic solar cells, based on regioregular poly(3-hexylthiophene-2,5-diyl) (rrP3HT) and [6,6]-phenyl-C_{61}-butyric acid methyl ester (PCBM), is analyzed via solid-state nuclear magnetic resonance (NMR). ^{1}H spin-lattice relaxation experiments of solid-state NMR clearly reveal that the phase-separated heterojunction structure develops on the order of several tens of nanometers in rrP3HT/PCBM blend films with thermal annealing at 150 °C. The development of the phase-separated structure explains the increase in the PCE for the solar cell system from 0.7% to nearly 3% through the thermal annealing. © *2011 American Institute of Physics*. [doi:10.1063/1.3662854]

Organic solar cells (OSCs) have attracted significant attention for their low-cost solar energy conversion. In extensive research on various OSCs, bulk heterojunction OSCs consisting of regioregular poly(3-hexylthiophene-2,5-diyl) (rrP3HT) and [6,6]-phenyl-C_{61}-butyric acid methyl ester (PCBM) have shown excellent performance as donors and acceptors, respectively.[1–4] One point of interest for the OSC systems is the effect of thermal annealing treatments. Padinger *et al.*[1] found that the power conversion efficiency (PCE) increases from 0.4% to 2.5% by annealing at 75 °C for 4 min. Ma *et al.*[2] reported a drastic increase in PCE from 0.8% to 5.1% by annealing at 150 °C for about 30 min. Similar trends have also been reported.[3,4] According to these studies, thermal annealing treatment is a very easy and inexpensive way to improve the performance of OSCs. Scientifically, it is important to understand what happens in the films during thermal annealing. Photoelectric conversion occurs via generation of excitons through the absorption of light, diffusion of excitons toward donor/acceptor interfaces, charge separation at the interface and formation of free carriers (holes and electrons), and transport of free carriers toward electrodes. During the processes, back electron transfer (recombination of holes and electrons) also occurs, which degrades the performance of OSCs. These processes occur at different size scales. Therefore, investigation of donor–acceptor structures at different size scales is important in understanding the efficiency of OSCs.

Solid-state nuclear magnetic resonance (NMR) is a useful tool to study local structures in organic materials.[5] Recently, it has also been applied to the analysis of materials for organic light-emitting diodes[6–8] and organic solar cells,[9–12] and it is expected to provide important knowledge on the abovementioned thermal annealing effect.[11–15] In this study, we investigated the change in the donor–acceptor structure in rrP3HT/PCBM systems during thermal annealing by spin-lattice relaxation measurements in solid-state NMR, which reveals the miscibility between rrP3HT and PCBM at different hierarchical levels. A clear relationship is found between the PCE of the OSC systems and the donor–acceptor structure revealed by solid-state NMR.

The OSCs were fabricated with a configuration of ITO (150 nm)/poly(3,4-ethylene dioxythiophene):poly(styrenesulfonate) (PEDOT:PSS) (40 nm)/rrP3HT:PCBM (1:1 w/w) (120 nm)/LiF (0.6 nm)/Al (100 nm). For annealed samples, the active layers were isothermally annealed at 150 °C for 5, 15, and 30 min in vacuum before depositing LiF and Al. The current density–voltage (J–V) characteristics were measured under 100 mW cm^{-2} white-light illumination (air mass 1.5 conditions). Samples for wide-angle x-ray diffraction (WAXD) and solid-state NMR experiments were prepared by drop casting a mixed solution of 1:1 (w/w) rrP3HT:PCBM in chloroform. Annealed samples were isothermally annealed at 150 °C for 5, 15, and 30 min under an N_2 atmosphere. Solid-state NMR measurements were conducted under a static magnetic field of 9.4 T. The ^{1}H spin-lattice relaxation times in the laboratory frame (T_{1H}) and those in the rotating frame ($T_{1\rho H}$) were measured to reveal miscibility on the order of several tens of nanometers and on the order of several nanometers, respectively.[13–15] For the system in this study, the size ranges were 16–40 nm and 2–7 nm, respectively, as shown later. Typical thicknesses of OSCs in the thin films are about 100 nm. Diffusion lengths of excitons in OSCs are considered to be ~20 nm. The length of the monomer unit of rrP3HT and the dimension of PCBM are roughly 0.4 and 1.0 nm, respectively. T_{1H} and $T_{1\rho H}$ experiments are important to understand the performance of OSCs because the dimensions analyzed in these experiments are related to percolation path lengths toward the electrodes, exciton diffusion lengths, charge separations (charge transfer), and back electron transfer (recombination of holes and electrons). The experimental details are given in Ref. 16.

Figure 1 shows J–V characteristics of the OSCs. Without annealing, the OSCs have a short-circuit current density (J_{sc}) of 2.42 mA/cm^2, an open-circuit voltage (V_{oc}) of 0.65 V, and a fill factor (FF) of 0.42, which results in PCE of 0.67%. The OSC characteristics drastically increase with annealing for only 5 min; J_{sc} and FF increase to 8.59 mA/cm^2 and 0.58, respectively. Although V_{oc} decreases to 0.53 V, the PCE

a)Author to whom correspondence should be addressed. Electronic mail: kaji@scl.kyoto-u.ac.jp.

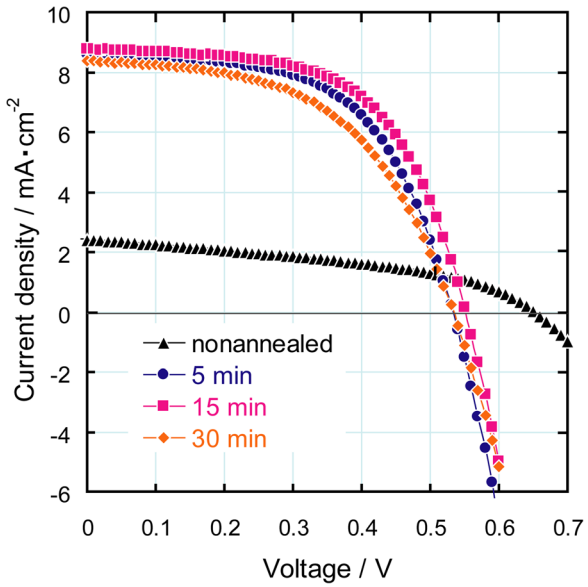

FIG. 1. (Color online) J–V curves obtained from rrP3HT/PCBM bulk heterojunction OSCs under AM 1.5 illumination at an irradiation intensity of 100 mW/cm^2. The annealing times are shown in the figure.

significantly increases to 2.65%. Compared with the drastic increase, the PCE values were similar to those obtained with further annealing (2.87% and 2.36% with 15 min and 30 min annealing, respectively).

The origin of the effect of the thermal annealing was investigated in WAXD and solid-state NMR experiments. Figure 2 shows the experimental WAXD profiles of the nonannealed and annealed samples. A definite change is found at a diffraction angle of ~19°; the diffraction becomes significantly sharp with the first 5 min of annealing. The diffraction at ~19° purely originates from the PCBM.[16] Therefore, the obvious change in Figs. 2(a) and 2(b) is related to some ordering of the PCBM. The ordering is considered to occur

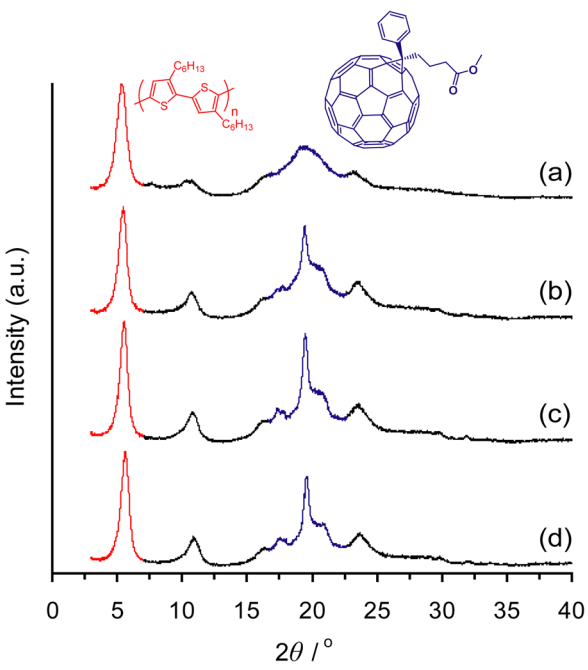

FIG. 2. (Color online) WAXD profiles of rrP3HT/PCBM blends: (a) as-cast, annealing at 150 °C for (b) 5 min, (c) 15 min, and (d) 30 min.

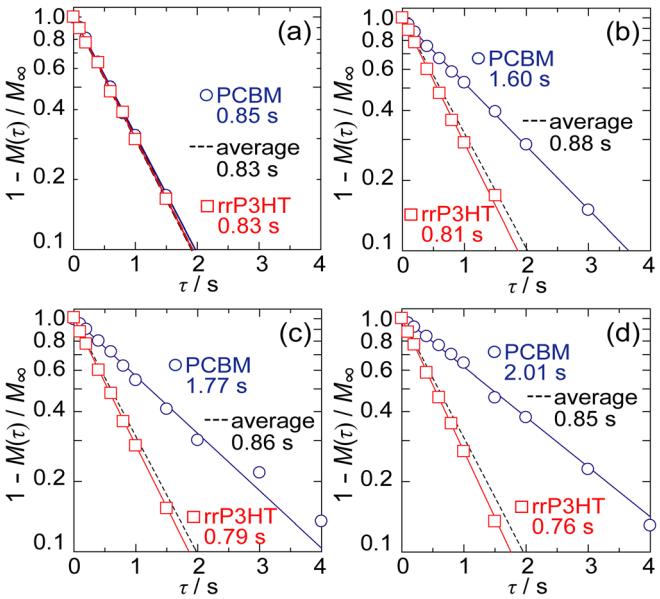

FIG. 3. (Color online) T_{1H} relaxation curves of rrP3HT (open squares) and PCBM (open circles) components in rrP3HT/PCBM blends; (a) as-cast, annealed at 150 °C for (b) 5 min, (c) 15 min, and (d) 30 min. The average relaxation curves for rrP3HT and PCBM are calculated[16] and shown as broken lines.

because of the formation of PCBM-rich domains resulting from the phase separation, as verified later in T_{1H} experiments. Compared with the drastic change, the change for rrP3HT is small. The diffractions at ~6°, which originate from rrP3HT, become only slightly sharp with annealing.

Figure 3 shows the results of T_{1H} experiments for the nonannealed and annealed samples. For the nonannealed samples (Fig. 3(a)), the T_{1H} relaxation behaviors of rrP3HT and PCBM agree with each other within experimental error; the T_{1H} values are 0.84 ± 0.01 s for both rrP3HT and PCBM. This indicates that rrP3HT and PCBM are mixed with each other on the order of several tens of nanometers. The size range, $\langle r \rangle$, is calculated using the diffusion equation $\langle r \rangle = \sqrt{6DT_{1H}}$, where D is the spin-diffusion coefficient; the domain size $\langle r \rangle$ is estimated to be 16–40 nm[16]. The agreement of the T_{1H} values for rrP3HT and PCBM indicates that the two constituents are homogeneously mixed within the 16–40 nm size range and no detectable domains larger than those are present in the nonannealed sample. The relaxation behaviors drastically change with isothermal annealing for only 5 min. As shown in Fig. 3(b), rrP3HT and PCBM in the sample annealed at 150 °C for 5 min have significantly different T_{1H} relaxation behaviors. The T_{1H} values of rrP3HT and PCBM are 0.81 and 1.60 s, respectively. This result clearly indicates that a phase-separated heterogeneous structure develops with annealing for only 5 min. The rrP3HT-rich and PCBM-rich domains larger than 16–40 nm form in the films. Further development of the phase separation is expected with annealing for 15 and 30 min (Figs. 3(c) and 3(d)). The T_{1H} values of rrP3HT (0.79 s and 0.76 s for 15 and 30 min of annealing) come close to that of pure rrP3HT (0.73 s for annealing at 150 °C for 30 min). Similarly, the T_{1H} values of PCBM (1.77 s and 2.01 s for 15 and 30 min of annealing) come close to that of pure PCBM (2.29 s for annealing at 150 °C for 30 min). However, the change from 5 to 30 min of annealing is small compared with that

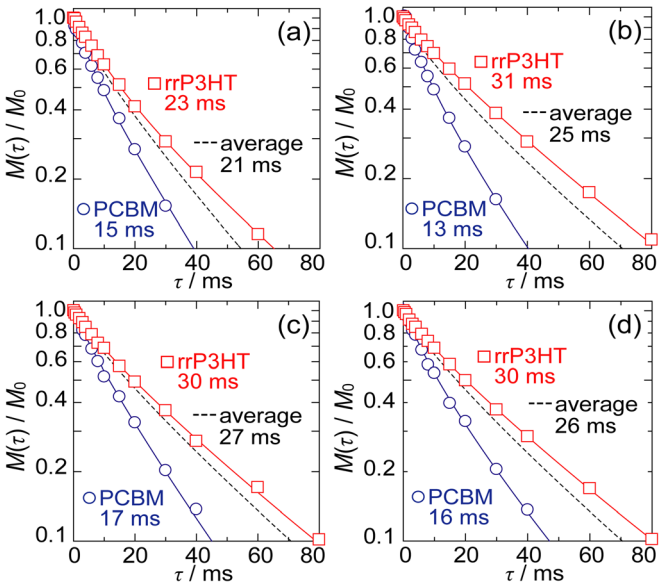

FIG. 4. (Color online) $T_{1\rho H}$ relaxation curves of rrP3HT (open squares) and PCBM (open circles) components in rrP3HT/PCBM blends; (a) as-cast, annealed at 150 °C for (b) 5 min, (c) 15 min, and (d) 30 min. The average relaxation curves for rrP3HT and PCBM are calculated[16] and shown as broken lines.

from 0 to 5 min. It is found that the structural change in this size range is closely related to the change in OSC performance shown in Fig. 1. The formation of rrP3HT-rich and PCBM-rich domains with 5 min annealing provides effective percolation paths for charge transport toward the electrodes. The phase separation is considered to contribute also to quenching the back electron transfer. These effects act as the improvement in cell performance, especially J_{sc}. Further phase separation would provide larger domains with decreased interfacial area, which may annihilate the excitons before they reach the donor–acceptor interfaces and also prohibit the generation of free carriers. However, the PCE does not decrease significantly with annealing up to 30 min and the undesirable effects are not observed. Such effects, which decrease the PCE, would appear at longer annealing times and/or higher annealing temperatures.

Figure 4 shows the results of $T_{1\rho H}$ experiments. In the experiments, the relaxation behavior cannot be explained by a single exponential decay, and a distribution of correlation times is required for the analysis. For the correlation time distribution, we use the Kohlrausch–Williams–Watts (KWW) function.[16,17] Different from the above T_{1H} experiments, rrP3HT and PCBM in the nonannealed sample had different $T_{1\rho H}$ relaxation behaviors (Fig. 4(a)). This indicates that rrP3HT and PCBM are phase separated even in the nonannealed samples on the order of several nanometers. The size range corresponding to the $T_{1\rho H}$ experiments was estimated to be 2–7 nm from the abovementioned spin diffusion equation, spin-diffusion coefficients, and the above $T_{1\rho H}$ values.[16] Figures 4(b)–4(d) show the results of $T_{1\rho H}$ experiments for the annealed samples. Although the $T_{1\rho H}$ value of rrP3HT changes from 23 to 31 ms with the first annealing of 5 min, the relaxation behaviors essentially remain the same, irrespective of annealing up to 30 min.[16] The $T_{1\rho H}$ values of the respective components in the blend samples are close to those of single-component samples annealed for 30 min (28 and 18 ms for pure rrP3HT and pure PCBM, respectively). This confirms that rrP3HT and PCBM are phase separated on the 2–7 nm scale irrespective of the annealing condition.

In summary, we investigated the change in the donor-acceptor heterojunction structure of rrP3HT/PCBM OSC systems during annealing mainly through solid-state NMR. The structures at different hierarchical levels, which are considered to be related to charge separation, back electron transfer, exciton diffusion, and charge transport, were analyzed in $T_{1\rho H}$ and T_{1H} experiments. The phase-separated structure analyzed in $T_{1\rho H}$ experiments does not significantly change with annealing. In contrast, it is clearly found in the T_{1H} experiments that a phase-separated heterojunction structure develops on the order of several tens of nanometers through thermal annealing of the rrP3HT/PCBM systems. The structure change provides percolated carrier paths and can accelerate charge transport in OSCs. The phase-separated structure is also expected to prohibit back electron transfer. This results in the improvement of the J_{SC} and hence the PCE.

This research was supported by the Japan Society for the Promotion of Science (JSPS) through the "Funding Program for World-Leading Innovative R&D on Science and Technology (FIRST Program)" initiated by the Council for Science and Technology Policy (CSTP). This work is partially supported by the New Energy and Industrial Technology Development Organization (NEDO) of the Ministry of Economy, Trade, and Industry (METI).

[1]F. Padinger, R. S. Rittberger, and N. S. Sariciftci, Adv. Funct. Mater. **13**, 85 (2003).
[2]W. L. Ma, C. Y. Yang, X. Gong, K. Lee, and A. J. Heeger, Adv. Funct. Mater. **15**, 1617 (2005).
[3]M. Al-Ibrahim, O. Ambacher, S. Sensfuss, and G. Gobsch, Appl. Phys. Lett. **86**, 201120 (2005).
[4]Y. Kim, S. Cook, S. M. Tuladhar, S. A. Choulis, J. Nelson, J. R. Durrant, D. D. C. Bradley, M. Giles, I. Mcculloch, C. S. Ha, *et al.*, Nature Mater. **5**, 197 (2006).
[5]K. Schmidt-Rohr and H. W. Spiess, *Multidimensional Solid-State NMR and Polymers* (Academic, London, 1994).
[6]H. Kaji, Y. Kusaka, G. Onoyama, and F. Horii, Jpn. J. Appl. Phys. **44**, 3706 (2005).
[7]H. Kaji, Y. Kusaka, G. Onoyama, and F. Horii, J. Am. Chem. Soc. **128**, 4292 (2006).
[8]Y. Nishiyama, T. Fukushima, K. Takami, Y. Kusaka, T. Yamazaki, and H. Kaji, Chem. Phys. Lett. **471**, 80 (2009).
[9]C. Y. Yang, J. G. Hu, and A. J. Heeger, J. Am. Chem. Soc. **128**, 12007 (2006).
[10]R. Mens, P. Adriaensens, L. Lutsen, A. Swinnen, S. Bertho, B. Ruttens, J. D'Haen, J. Manca, T. Cleij, D. Vanderzande, and J. Gelan, J. Polym. Sci., Part A: Polym. Chem. **46**, 138 (2008).
[11]R. C. Nieuwendaal, C. R. Snyder, R. J. Kline, E. K. Lin, D. L. VanderHart, and D. M. DeLongchamp, Chem. Mater. **22**, 2930 (2010).
[12]H. Kaji, H. Hayashi, T. Yamada, M. Fukuchi, S. Fujimura, M. Ueda, S. Kang, T. Umeyama, Y. Matano, and H. Imahori, Appl. Phys. Lett. **98**, 113301 (2011).
[13]V. J. McBrierty, D. C. Douglass, and T. K. Kwei, Macromolecules **11**, 1265 (1978).
[14]X. Zhang, K. Takegoshi, and K. Hikichi, Polym. J. **23**, 87 (1991).
[15]A. Asano, K. Takegoshi, and K. Hikichi, Polym. J. **24**, 555 (1992).
[16]See supplemental material at http://dx.doi.org/10.1063/1.3662854 for WAXD profiles of pure rrP3HT and pure PCBM, pulse sequences for T_{1H} and $T_{1\rho H}$ experiments, estimation of domain sizes, and effect of molecular dynamics.
[17]G. Williams, D. C. Watts, S. B. Dev, and A. M. North, Trans. Faraday Soc. **67**, 1323 (1971).